Delft University of Technology

Finite Element Analysis and Experimental Validation of Eddy Current Losses in Permanent Magnet Machines with Fractional-Slot Concentrated Windings

Wang, Xuezhou; Liu, Dong; Lahaye, Domenico; Polinder, Henk; Ferreira, Jan A.

Finite Element Analysis and Experimental Validation of Eddy Current Losses in Permanent Magnet Machines with Fractional-Slot Concentrated Windings

Xuezhou Wang*, Dong Liu*, Domenico Lahaye**, Henk Polinder* and Jan A. Ferreira*

*Department of Electrical Sustainable Energy, Delft University of Technology, Mekelweg 4, 2628 CD, Delft, the Netherlands

**Delft Institute of Applied Mathematics, Delft University of Technology, Mekelweg 4, 2628 CD, Delft, the Netherlands

Abstract—**Permanent-magnet machines with fractional-slot concentrated windings are easy to manufacture. Their popularity therefore is steadily increasing. Without a proper design, however, the induced eddy-current losses in the solid rotor get rather high. The modeling and the prediction of eddy-current losses for these machines are thus very important during the design process. This paper focuses on the finite-element analysis and the experimental validation of eddy-current losses for this kind of machine with a small axial length. Two-dimensional and three-dimensional transient finite-element models are developed for computing the eddy-current losses. The rotor motion is taken into account using an Arbitrary Lagrangian-Eulerian formulation. The total iron losses are measured experimentally and a method to separate the rotor iron losses from the total iron losses is presented. The validation results show that the two-dimensional finite-element model overestimates the losses due to the end-effects being neglected. The three-dimensional model agrees much better with the measurements in both no-load and on-load operations.**

Index Terms—**Concentrated winding, eddy current losses, experimental validation, permanent magnet machine.**

I. INTRODUCTION

Permanent magnet (PM) machines with fractional-slot concentrated stator windings have simple coils which can be wound easily and fast. This advantage allows for automatic winding processes resulting in a higher cost-effectiveness [1]. However, the critical drawback with fractional-slot concentrated windings is that the space harmonics in the magneto-motive force (MMF) produce considerable eddy-current losses in the conductive parts (e.g. PMs and rotor yoke) [2]. These high losses could result in a high temperature that demagnetizes the PMs. Therefore, it is crucially important to understand the eddy-current better and predict the eddy-current losses during the design process.

The eddy-current in this kind of PM machine is mainly caused by stator slotting [3], [4], space harmonics in MMF due to winding distribution [5], [6] and the time-harmonics of MMF due to non-sinusoidal currents [7], [8]. In this paper, the machine studied is running as a synchronous generator producing power to a resistive load. For simplicity, we assume that the armature phase current is purely sinusoidal. Therefore, this paper only takes into account the first two causes for the eddy-current losses.

Analytical models and finite element (FE) methods are commonly used for the analysis and prediction of eddy-current losses [9]. Most of the analytical models are two-dimensional and make various assumptions. In [2] and [10] the models are linear and the stator MMF is represented by an equivalent current density sheet. The induced eddy-currents are assumed to be resistance limited and the eddy-current losses are calculated from the magneto-static solutions [2], [5]. That means the influence of the reaction field due to eddy-current is neglected. In addition, it is not straightforward to extend these models to take the complexity into account.

FE methods can easily take into account the complicated geometries and the non-linear material properties to overcome the analytical models' shortcomings. Two-dimensional (2D) FE models have been widely used to investigate the eddy-current losses in the surface-mounted PM machines [11], [12] or the interior PM machines [13]. With the developing computer technologies, three-dimensional (3D) FE models are drawing more attention to take into account the end-effect. Papers have worked on the computationally efficient approaches for 3D FE model for the purpose of saving the computing resource. For example, the stator MMF could be modeled by a current sheet as a special boundary which obtained from the 2D analytical model [14] or the 2D magneto-static FE model [15]. Furthermore, in order to consider any certain harmonic order, several 3D magneto-static solutions at different rotor positions can be used to calculate the eddy-current losses based on the space-time transformations [16].

Analytical models are usually validated by the FE analysis [11] since the FE models are more close to the reality. However, few papers have compared the calculation results with the measurements due to the difficulty in measuring the eddy-current losses. An effort has been made to validate a 2D FE model by an experiment, but the validation shows obvious deviations between the 2D FE calculation results and the measurements [12], [17]. The reasons for such deviations remain to be further investigated.

This paper extends the work in [17] by building a 3D transient FE model, including rotor motion, to better understand the deviation between the 2D FE predictions
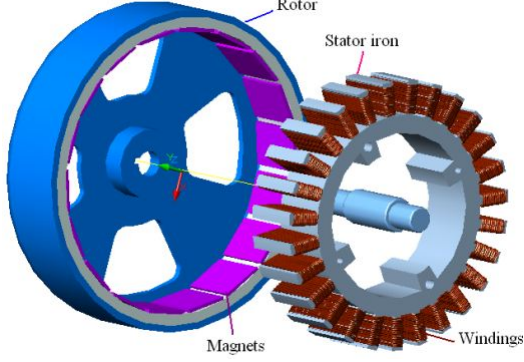
Fig. 1. Prototype of the concentrated winding machine studied [12]

TABLE I
MAIN SPECIFICATIONS OF THE MACHINE STUDIED

Description	Unit	Machine parameter
Rotor radius	[mm]	97
Stator radius	[mm]	90
Air-gap length	[mm]	2
Magnet thickness	[mm]	5
Rotor back-iron thickness	[mm]	15
Axial length	[mm]	45
Rated power	[kW]	9
Number of phase		3
Number of slots		27
Number of poles		18
Number of turns per coil		10
Remanent flux density of magnet (NdFeB) at $20°$C	[T]	1.2
Conductivity of magnet	[S/m]	0.76×10^6
Conductivity of rotor back-iron	[S/m]	5×10^6
Relative permeability of magnet		1.05

and the measurements. A detailed procedure of measuring the total iron losses is described. A method to separate the rotor iron loss from the total iron losses is presented. It combines the 2D FE simulations and the manufacturer's data sheet for the iron laminations. The phase angle between the electro-motive force (EMF) and the applied phase current is taken into account and it is found influential on the accuracy of predicting eddy-current losses. Both the 2D and 3D FE models are validated by the experimental measurements.

This paper starts with a short description of the machine under study. Next, the equations of 3D electromagnetic field and eddy-current losses and the method dealing with rotor motion are presented. The 3D transient FE model is then built and implemented in COMSOL Multiphysics. Subsequently, the principle and the set-up to measure and separate the eddy current losses are demonstrated, followed by the comparisons between the FE simulation results and the measurements. The conclusions are drawn in the end.

II. MACHINE UNDER STUDY

The machine studied is shown in Fig. 1. It has 27 slots in stator, 18 PM poles in rotor and a small axial length. The main specifications are given in Table I.

III. THREE-DIMENSIONAL TRANSIENT FE MODELING

The electromagnetic field equations of a 3D transient FE model are derived in this section. The method dealing with the rotor motion is illustrated, as well as the formulation of the eddy current losses.

A. Electromagnetic Field Equations

Considering the motion effect, the electromagnetic field equation can be written as:

$$\nabla \times (H - \mu^{-1}B_r) = \sigma(E + v \times B) + J_e, \quad (1)$$

where H is the magnetic field intensity, μ the permeability of the material, B_r the remanent flux density of permanent magnets, σ the electric conductivity, E the electric field intensity, v the velocity of the medium with respect to the

reference system, B the magnetic flux density and J_e the externally applied current density.

The divergence-free condition for the magnetic flux density B is ensured by expressing B in terms of the magnetic vector potential A as:

$$B = \nabla \times A. \quad (2)$$

Together with constitutive material equations, the completed field equation to be solved can be written as:

$$\nabla \times (\mu^{-1}(\nabla \times A - B_r)) - \sigma v \times (\nabla \times A) = -\sigma\frac{\partial A}{\partial t} + J_e, \quad (3)$$

In order to get an unique magnetic flux density, we must specify both its divergence and its curl, but Equation (2) leaves the divergence undetermined. Therefore, Coulomb gauge is necessary:

$$\nabla \cdot A = 0. \quad (4)$$

In the case that there is no current in some media (e.g surrounding air), Equation (1) reduces to:

$$\nabla \times H = 0. \quad (5)$$

It is easier to introduce magnetic scalar potential V_m to represent the solution for the Equation (5):

$$H = -\nabla V_m. \quad (6)$$

Then the equation to be solved can be written as:

$$\nabla \cdot (-\mu\nabla V_m) = 0. \quad (7)$$

In our 3D FE models, Equation (3) and Equation (7) are solved in a coupled fashion. The magnetic vector potential is applied in conductive domain (PMs and rotor back-iron) while the magnetic scalar potential is used in the non-conductive region (surrounding air). This technique effectively reduces the number of DOFs and simplifies the simulation of the moving boundary.

B. Modeling Motion

The algorithms of continuum mechanics usually make use of two classical descriptions of motion: the Lagrangian description and the Eulerian description. In Lagrangian algorithms, each individual node of the computational mesh follows the associated material particle during motion. In Eulerian algorithms, the computational mesh is fixed and the continuum moves with respect to the grid. A more flexible approach is the Arbitrary Lagrangian-Eulerian (ALE) description in which the nodes of computational mesh move with the continuum in normal Lagrangian fashion, or are held fixed in an Eulerian manner [18].

In rotating machine situation, we can use a reduced ALE method in which Eulerian algorithms is applied in the stationary part (stator) with stationary coordinate system represented by $x_j(x, y, z)$. Lagrangian algorithms is applied in the motion part (rotor) with motion coordinate system represented by $X_i(X, Y, Z)$. As an example, we evaluate the magnetic vector potential A at particle X_i which locates x_j in stationary coordinate system. It can be described in the motion coordinate system and the stationary coordinate system respectively:

$$\begin{cases} A = A_X(X_i, t), & \text{in motion coordinate system} \\ A = A_x(x_j, t), & \text{in stationary coordinate system.} \end{cases}$$
$$(8)$$

Although two coordinate systems are used, the total time derivative of the quantity A should be equal:

$$\frac{DA_X}{Dt} = \frac{DA_x}{Dt}, \qquad (9)$$

and therefore

$$\frac{\partial A_X}{\partial t}\Big|_{X_i} + \frac{dX_i}{dt}\frac{\partial A_X}{\partial X_i}\Big|_t = \frac{\partial A_x}{\partial t}\Big|_{x_j} + \frac{dx_j}{dt}\frac{\partial A_x}{\partial x_j}\Big|_t. \quad (10)$$

We already know that $\frac{dX_i}{dt} = 0$ in motion coordinate system while $\frac{dx_j}{dt} = v_j$ in stationary coordinate system. We therefore have that:

$$\frac{\partial A_X}{\partial t}\Big|_{X_i} = \frac{\partial A_x}{\partial t}\Big|_{x_j} + v_j\frac{\partial A_x}{\partial x_j}\Big|_t. \qquad (11)$$

It is not difficult to see the rotor seems standstill if we give the same rotational speed to the calculating mesh nodes. However, according to the Equation (11), the motion has been taken into account essentially. It also means the calculating grids have no distortion. Therefore, the space derivative of a quantity meets with the following relationship:

$$\triangle' = \triangle, \qquad (12)$$

where $\triangle'$ and $\triangle$ represent Laplacian in motion coordinate system and stationary coordinate system respectively [19]. By using ALE method, the field equations solved in the rotor and the stator have the same form which come from Equation (3):

$$\nabla \times (\mu^{-1}(\nabla \times A - B_r)) = -\sigma\frac{\partial A}{\partial t} + J_e. \qquad (13)$$
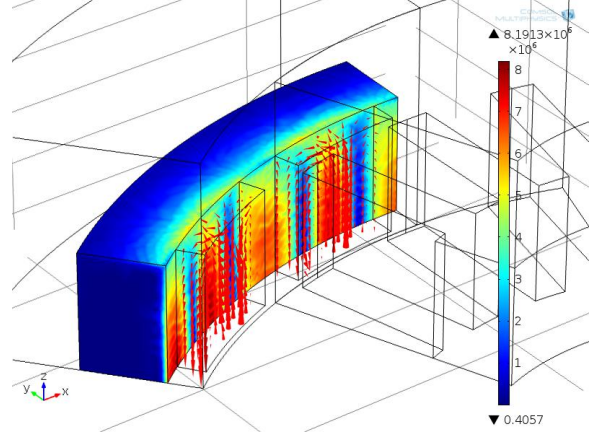

Fig. 2. Eddy-current distribution in 3D FE transient model at t = 2ms.

C. Rotor Eddy Current Loss Formulation

In Cartesian coordinate system, J_x, J_y and J_z represent the eddy-currents in x, y and z directions respectively. The eddy-current losses can be calculated as the following equation:

$$P_r = \iiint_V (\frac{|J_x|^2}{\sigma_x} + \frac{|J_y|^2}{\sigma_y} + \frac{|J_z|^2}{\sigma_z})dV, \qquad (14)$$

where V is the volume of the solid conductive parts and σ_x, σ_y and σ_z are electric conductivities in the coordinate directions. In case of an isotropic material, we have that $\sigma_x = \sigma_y = \sigma_z$.

D. Implementation

Fig. 2 shows the 3D FE model of the machine studied, including rotor motion. Utilizing symmetrical property, only a section corresponding to one ninth in transverse section and half in axial direction is simulated to save simulation time. The ALE method (moving mesh method in COMSOL Multiphysics [20]) is used to take into account rotor motion. The FE model is divided into two parts, namely the motion part (rotor) and the stationary part (stator) linked together by using symmetrical identity pairs.

The tetrahedron element is applied in 3D model, resulting in 64369 elements and 237794 DoFs. Meshes in the non-conductive domain where the magnetic scalar potential is applied are set based on our experiences with the FE model. In the conductive domain, the meshes should be chosen according to the skin depth to consider this effect sufficiently. The skin depth in the rotor yoke is so small that an extremely fine mesh is needed. Our model did not apply a sufficiently fine mesh in this region because of the memory problems. Fortunately, as the results will show, the eddy-current losses are dominant in the PMs and the mesh used is sufficiently fine in the corresponding part of computational domain. Therefore, the simulation results can still give a meaningful prediction of losses although the meshes in the yoke are not very fine.
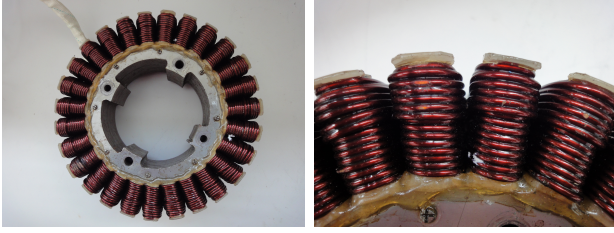
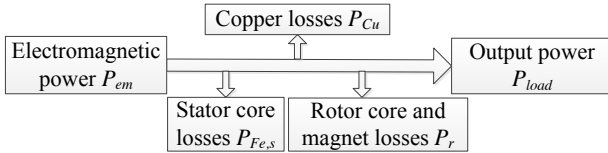Fig. 3. Open-slot stators used in experimental measurements

Fig. 4. Modified power flow model of a PM synchronous generator

Fig. 5. Setup for experimental tests

Connected with the spring balance

Fig. 6. Connection of the spring balance to the stator

IV. EXPERIMENTAL VALIDATION

An open-slot stator (shown in Fig. 3) is used in the experiments to do the validation of the FE model for the open-slot stator situation. The principle and the set-up are illustrated followed by comparisons between the simulations and the measurements.

A. Principle of Experimental Measurements

The PM machine in rotary tests is running in the mode of synchronous generator. The power flow of a PM synchronous generator with its prime mover drive is illustrated in [21]. Since the prime mover and mechanical losses are difficult to measure precisely, it is more reliable that we skip the measurement of the prime mover and mechanical losses and directly measure the electromagnetic power in the air gap as the input power to the PM generator. The impact of prime mover and mechanical structure could thus be minimized. Hence the model of power flow is modified as shown in Fig. 4. In principle, using both the two models should give the same result, but we choose the modified model for the experiments because it is easier to implement. The mechanical loss coming from the bearing between the stator and the shaft is not considered in the power flow model because it has been checked to be negligible at various speeds by experiments.

The setup for the experimental test is shown in Fig. 5. The DC motor acts as the prime mover and the PM machine studied runs as a synchronous generator. The electromagnetic power P_{em} on the shaft delivered from the prime mover is measured by a spring balance which is connected to the stator and gives the magnitude of the shear force F_{em} on the outer surface of the stator. The value of P_{em} can be obtained as:

$$P_{em} = \omega F_{em} l, \qquad (15)$$

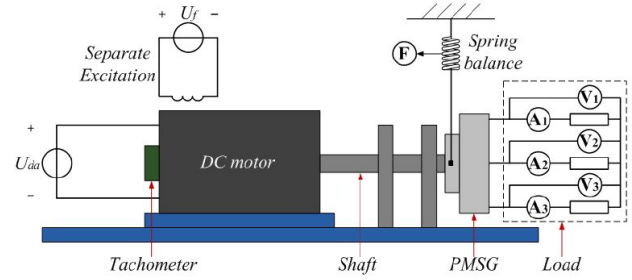where ω is the rotational speed and l is the force arm between the stator center and the point where the force 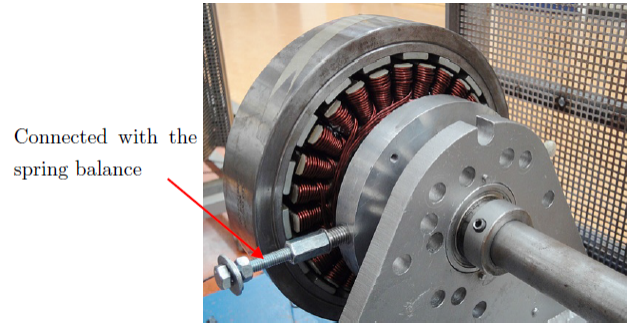measured. Note that the spring balance is fixed in the position that the force Fem is perpendicular to the distance r in the same plane as demonstrated in Fig. 6.

This electromagnetic power equals to the sum of copper losses, stator iron losses, rotor eddy-current losses and the electrical output power in the generator. Therefore, the sum of the rotor eddy-current losses P_r computed using Equation (14) and the stator iron losses $P_{Fe,s}$ can be easily obtained by:

$$P_r + P_{Fe,s} = P_{em} - P_{Cu} - P_{load}, \qquad (16)$$

where P_{Cu} is the copper loss when the generator is loaded with a purely resistive three-phase load P_{load}.

B. Separation of Rotor Iron Loss

In order to separate the rotor iron loss, a method that combines 2D FE simulations with manufacturer's data sheet is used to estimate the stator iron losses. The AC flux densities are computed by 2D FE simulations throughout the entire stator. The local high flux densities can be taken into account by doing so. The ferromagnetic material used for the stator is M-19-29-Ga non-oriented silicon steel. Fig. 7 gives the relation between iron core losses per unit mass and the peak flux density at different frequencies. Based on the 2D transient FE results, the flux density at any position in stator core domain can be obtained as a function of time. By applying time FFT, it is straightforward to figure out the amplitude and the corresponding frequency of the dominant flux density. Then the stator core losses can be predicted by look-up in Fig. 7. Fig. 8 gives a 2D distribution of the magnetic fields, as well as the flux lines, at one time moment.
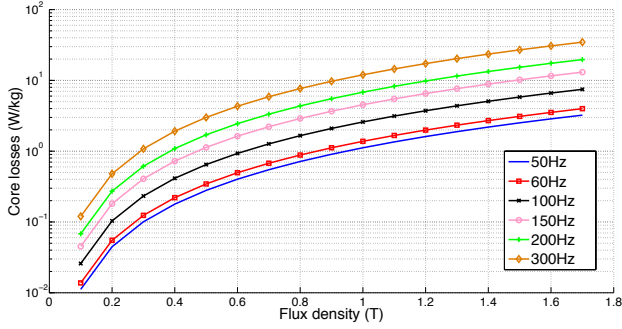
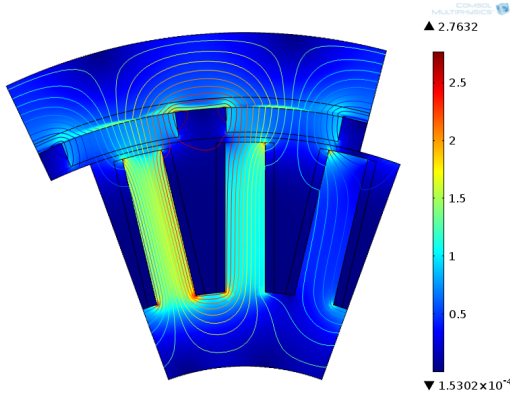Fig. 7. Iron loss as a function of flux density at different frequencies

Eddy current	PM		Rotor yoke	
losses (W)	3D FEM	2D FEM	3D FEM	2D FEM
P_{J_x}	8.91	-	5.53	-
P_{J_y}	1.37	-	3.29	-
P_{J_z}	97.25	144.32	34.95	41.28
P_r	107.53	144.32	43.77	41.28
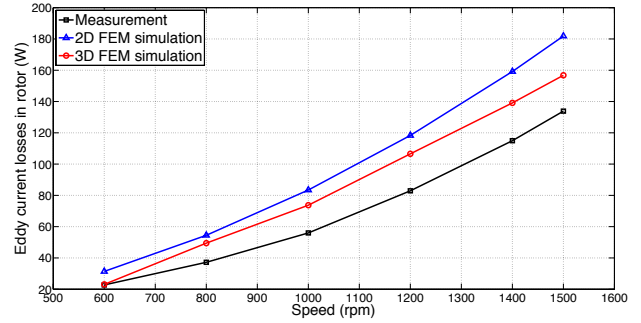
Fig. 10. Rotor eddy-current losses in on-load case with zero phase angle

Fig. 8. 2D magnetic fields and flux lines
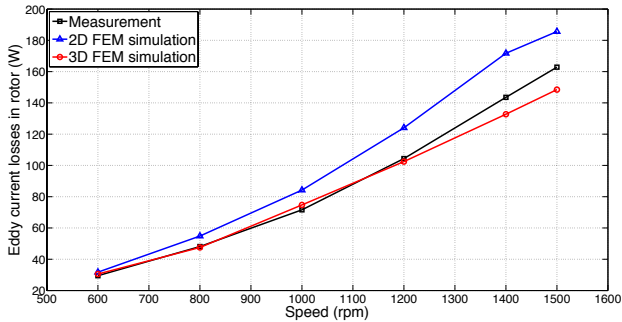

Fig. 11. Phase diagram of PM generator

Fig. 9. Rotor eddy current losses in no-load case

C. Comparison between Simulations and Measurements

Fig. 9 shows the eddy-current losses in rotor with respect to its rotational speed in no-load case. The losses increase with increasing speeds as the frequency goes up. The 3D FE model gives a more accurate prediction. The reason is that, in 2D FE model, the influence of end-effects is neglected which is actually significant in a short axial machine.

For a further explanation, Table II gives the FE simulation results of no-load case in which the eddy-current losses calculated by Equation (14). We can see that, for both the PM and the rotor yoke, the z-component of the eddy-current losses in the 3D model dominates the other two components. The 2D model neglects the end-effects and overestimates the eddy-current losses. In addition, it is clear that the eddy-current losses in PMs dominate the
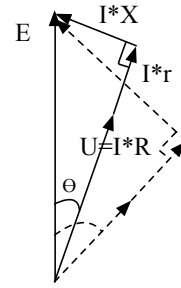
total rotor eddy-current losses. It verifies that we shall pay more attention to reduce the eddy-current loss in the PMs for less total losses and preventing the PMs demagnetization. Furthermore, Table II shows that the computed eddy-current losses P_r in the PMs is larger in the 2D FE model than in the 3D FE model. The opposite situation could occur for the eddy-current losses in the rotor yoke. We relate this to the mesh distribution as numerical experiments have shown that the eddy-current losses in the rotor yoke increase in case that a coarser mesh is used.

Fig. 10 shows the rotor eddy-current losses with respect to the speed in on-load case (10A). Initially, the applied current and the emf are assumed to be in phase since the angle θ between the current and the emf is small in reality. However, the following results show that θ (shown in Fig. 11) does have an influence on the accuracy of losses prediction. Comparing with the no-load case, the measured losses decrease, because the armature reaction weakens the main field created by the PMs and lowers the eddy-current losses. But the FE models do not give the same trend.
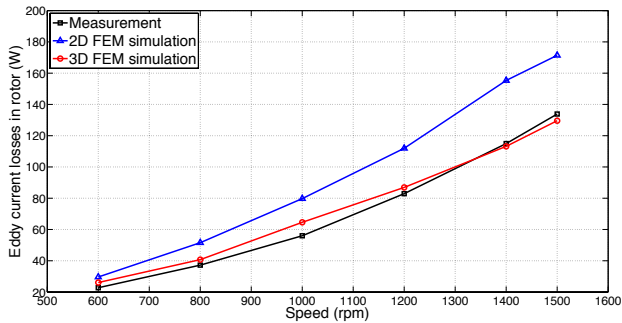
Fig. 12. Rotor eddy-current losses in on-load case with non-zero phase angle

The angle θ can be estimated by the measured terminal voltages in no-load and on-load case according to Fig. 11, in which r is the winding resistance of a phase and R is the load resistance. The dashed line in Fig. 11 shows that θ varies with the load level. This angle can be considered in the applied current density J_e in the FE models. Fig. 12 gives the rotor losses with respect to the speed after taking the phase angle θ into account. Simulation results give a good prediction of the losses, as well as the trend when the generator is loaded. The 3D FE model agrees well with the measurements like that in no-load case.

V. CONCLUSION

This paper presents a transient three-dimensional finite element model for the assessment of eddy-current losses in permanent-magnet machines with concentrated windings. Rotor motion is taken into account by using a reduced ALE formulation. The detailed procedure to measure the total iron losses and the method to separate the stator iron loss are descried. By validating with the experimental measurements, the results show that the end-effects cannot be neglected especially in the machine with a short axial length. The 3D model presented agrees well with the measurements. It also indicates that eddy-current losses in permanent-magnets occupy the major part of rotor losses and therefore needs more attention during the design. Actually, according to the results, we can see the rotor eddy-current losses are big (about 140W) in this PM machine. Measures to reduce these losses are therefore required. Furthermore, in order to model the characteristics accurately, the phase angle between the emf and the applied current needs to be considered in FE model according to its load level. Finally, because of the measurement validations, we are confident that the presented model constitutes a valuable tool in the detailed analysis and design of these machines.

REFERENCES

[1] A. M. EL-Refaie. *Fractional-Slot Concentrated-Windings Synchronous Permanent Magnet Machines: Oppurtunities and Challenges,* IEEE Trans. Industrial Electronics, vol.57, no.1, pp.107-121, Jan 2010.

[2] H. Polinder, M. J. Hoeijmakers, M. Scuotto. *Eddy-Current Losses in the Soild Back-Iron of PM Machines for different Concentrated Fractional Pitch Windings,* Electric Machines & Drives Conference. IEMDC '07. IEEE International, vol.1, no., pp.652-657, May 2007.

[3] K. Ng, Z. Q. Zhu and D. Howe. *Open-Circuit Field Distribution in Brushless Motor with Diametrically Magnetised PM rotor, Accounting for Slotting and Eddy Current Effects,* IEEE Trans. Magnetics, vol.32 no.5, pp.5070-5072, Sept 1996.

[4] G. Dajaku, D. Gerling. *Stator slotting effect on the magnetic field distribution of salient pole synchronous permanent-magnet machines,* IEEE Transactions on Magnetics, vol.46, no.9, pp.3676-3683, Sept 2010.

[5] K. Atallah, D. Howe, P. H. Mellor and D. A. Stone. *Rotor Loss in Permanent-Magnet Brushless AC Machines,* IEEE Transactions on Industry Applications, vol.36, no.6, pp.1612-1618, Nov/Dec 2000.

[6] H. Toda, Z. Xia, J. Wang, K. Atalla and D. Howe. *Rotor Eddy-Current Loss in Permanent Magnet Brushless Machines,* IEEE Transactions on Magnetics, vol.40, no.4, pp.2104-2106, July 2004.

[7] F. Deng, T. W. Nehl. *Analytical Modeling of Eddy-Current Losses Caused by Pluse-Width-Modulation Switching in Permanent-Magnet Brushless Direct-Current Motors,* IEEE Transactions on Magnetics, vol.34, no.5, pp.3728-3736, Sept 1998.

[8] Z. Q. Zhu, K. Ng, N. Schofield, D. Howe. *Improved analytical modelling of rotor eddy current loss in brushless machines equipped with surface-mounted permanent magnets,* IEE Proc.-EPA, vol.151, no.6, pp.641-650, 2004.

[9] A. Jassal, H. Polinder, J. A. Ferreira. *Literature Survey of Eddy-Current Loss Analysis in Rotating Electrical Machines,* IET Electric Power Applications, vol.6, pp.743-752, 2012.

[10] Z. J. Liu, A. Vourdas, K. J. Binns. *Magnetic Field and Eddy Current Losses in Linear and Rotating Permanent Magnet Machines with a Large Number of Poles,* IEE Proc. A Science, Measurement and Technology, vol.138, pp.289-294, 1991.

[11] A. Jassal, H. Polinder, D. Lahaye, J. A. Ferreira. *Analytical and FE Calculation of Eddy-Current Losses in PM Concentrated Winding Machines for Wind Turbines,* 2011 IEEE International Electrical Machine & Drives Conference (IEMDC), 2011.

[12] Hung Vu Xuan, D. Lahaye, M. J. Hoeijmakers, H. Polinder, J. A. Ferreira. *Studying Rotor Eddy Current Loss of PM Machines Using Nonlinear FEM Including Rotor Motion,* Electrical Machines (ICEM), 2010 XIX International Conference on, vol., no., pp.1-7, Sept. 2010.

[13] S. H. Han, T. M. Jahns and Z. Q. Zhu. *Analysisi of Rotor Core Eddy-Current Losses in Interior Permanent-Magnet Synchronous Machines,* IEEE Trans. Industry Applications, vol.46, no.1, Jan/Feb 2010.

[14] J. Wang, F. Papini, R. Chin, W. M. Arshad, H. Lendenmann. *Computationally efficient approaches for evaluation of rotor eddy current loss in permanent magnet brushless machines,* Electrical Machines and Systems,ICEMS 2009, International Conference on, Nov. 2009

[15] M.van der Geest, J. J. Wolmarans, H. Poliner, J. A. Ferreira, D. Zeilstra. *Rotor losses in laminated magnets and an anisotropic carbon fiber sleeve,* Power Electronics, Machines and Drives (PEMD 2012), 6th IET International Conference on, March 2012

[16] P. Zhang, G. Y. Sizov, J. He, D. M. Ionel, N. A. O. Demerdash. *Calculation of magnet losses in concentrated-winding permanent-magnet synchronous machines using a computationally efficient finite-element method,* IEEE Trans. Industry Applications, vol.49, no.6, Novermber 2013

[17] D. Liu, A. Jassal, H. Polinder, J. A. Ferreira. *Validation of Eddy Current Loss Models for Permanent Magnet Machines with Fractional-Slot Concentrated Windings,* Electric Machines & Drives Conference (IEMDC), 2013 IEEE International, vol., no., pp.12-15, May 2013

[18] J. Donea, A. Huerta, J. -Ph. Ponthot and A. Rodríguez-Ferran. *Arbitrary Lagrangian-Eulerian Methods,* Encyclopedia of computational mechanics, John Wiley and Sons, 2004

[19] T. Huang, J. Ruan, Y. Zhang, Y. Gan, M. Sun and H. Liu. *Research on the Time Steeping Element Method for Solving the Transient Motion Electromagnetic Problems,* Proceedings of the CSEE, vol.6, no., pp.168-175, Feb. 2013

[20] COMSOL Multiphysics. *version 4.3,* COMSOL AB, 2012

[21] S. J. Chapman. *Electric Machinery Fundamentals,* 3rd edition, McGraw-Hill Education, 1999